EFFECT OF PREBUCKLING AND EDGE SUPPORT ON BIFURCATION BUCKLING OF TORISPHERE, CYLINDER AND CONE

O. Ifayefunmi[1*]

[1]Faculty of Engineering Technology,
Universiti Teknikal Malaysia Melaka,
76100, Durian Tunggal, Melaka, Malaysia

ABSTRACT

This paper considers the buckling behaviour of commonly used shell structures in the offshore and oil industry. Three types of shells subjected to external pressure were examined, and they are: (i) torispheres, (ii) circular cylinders and (iii) truncated cones. It is assumed that shells are made from steel and the material is modeled as elastic material behaviour. Buckling strength for cases of different prebuckling/perturbation load and different edge support were obtained. In the case of transfer, results indicate that the magnitude of prebuckling/pertubation load has a significant effects on the bifurcation pressure. Whilst, changing the edge support has no effect on the buckling load. For the case of circular cylinder and cone, numerical calculation reveals that the magnitude of the prebuckling/pertubation load does not affect the bifurcation pressure. Whereas, in the case of different edge support, for a convergent solution to be obtained, the edge support must be either pinned or fully clamped at both ends. This is purely numerical study but the results of bifurcation pressure were compared with available data in open literature.

KEYWORDS*: Bifurcation buckling; Elastic modelling; External pressure; Torisphere; Circular cylinder; Truncated cone*

1.0 INTRODUCTION

Shell structures are major structural components used in most engineering applications i.e., automobile, building, marine, offshore and oil industries. The most commonly used shell structures in the offshore and oil industries are: torispheres, circular cylinders, truncated cones etc. They find applications in pressure vessels, onshore and offshore pipelines, offshore platforms legs, storage tankers, floating production storage and offloading (FPSO) and flow reducer in pipelines. When in use, they are subjected to various loading conditions such as external

* Corresponding author email: olawale@utem.edu.my

pressure, internal pressure, axial compression, bending, torsion, etc., or combined loading, i.e., axial compression and torsion, axial compression and external or internal pressure, torsion and external pressure or internal pressure, etc.

One of the major factors that limit the extent to which these structures can be loaded is static stability such as buckling. References to earlier works on shell buckling can be found in (Nash, 1960; Noor, 1990; Samuelson & Eggwertz, 1992; Sechler, 1974; Singer, 1999; Singer et al., 2002; Teng & Rotter, 2004).

The effects of buckling on major offshore structures are shown in Figure 1. This can be catastrophic and costly, thereby resulting in some of the following: (a) loss of life, (b) loss of properties and belongings, (c) costly financial implication, (d) loss of time, and (e) pollution. Several works have been carried out in order to investigate the buckling behavior of this shell structures but the effects of prebuckling/perturbation load during the buckling analysis has not been mentioned (Blachut, 1987, 2011, Blachut and Jaiswal, 1999, Fakhim et al., 2009 and Galletly et al., 1987). Recent result about the variability of different boundary condition for plastic collapse of cones subjected to external pressure or axial compression can be found in (Ifayefunmi, 2011; Ifayefunmi and Blachut, 2011). There is a special need to investigate the effect of boundary condition at the ends of this shell structures during useful application. This will highlight the extent of damage that may be caused by the loss of structural stability and the mechanical behaviour of such shells subjected to external loads with their associated buckling /failure modes.

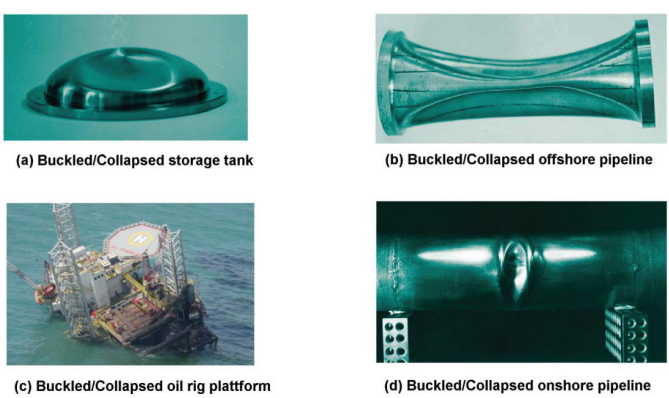

Figure 1. Typical effects of buckling of offshore/onshore structures

This technical challenge has spawned significant interest in the author to study the effects of preloading/perturbation load and variability of boundary conditions at the ends of these shell structures, i.e., torisphere, circular cylinder and cone subjected to external pressure. However, to successfully carry out buckling analysis on these shell components, it is important to carefully study and understand the behavior of such shell structures which are being examined (Kyriakides & Corona, 2007).

In this research work, bifurcation buckling behavior of three major shell structures used in the offshore industry, i.e., torispheres, circular cylinders and truncated cones were analyzed using ABAQUS finite element code (Habbitt et al., 2006). The effect of using different prebuckling/perturbation magnitude as well as the influence of variability of edge support on the bifurcation pressure of such structures is highlighted.

2.0 BACKGROUND INTO ELASTIC STABILITY OF SHELL STRUCTURES

Elastic buckling failure of three selected shell geometries under external pressure will be analyzed in this section. This is done in order to provide a general overview of the effect of preloading/perturbation and variability of edge support for elastic bifurcation buckling behavior of commonly encountered shell components in offshore applications.
Bifurcation buckling loads of the structures were obtained through eigenvalue buckling procedure using subspace solver. During the eigenvalue buckling analysis, the model was first preloaded with 'a dead load' using non-linear static analysis, and then the buckle step was evoked on the model with 'a live load' which is a fraction of the dead load. The buckling loads were calculated relative to the base state of the structure. The lowest eigenvalue computed was of interest because it is directly related to the bifurcation buckling load of the structures. The critical buckling load, $p_{\text{bifurcation}}$, can then be represented with the equation below (Habbitt et al., 2006):

$$p_{\text{bifurcation}} = \mathrm{P}^{\mathrm{N}} + \lambda_{\mathrm{i}}\mathrm{Q}^{\mathrm{N}} \tag{1}$$

where, P^{N} is the dead load (prebuckling load), Q^{N} is the live load (perturbation load) and λ_{i} is the lowest eigenvalue obtained from the eigenvalue buckling analysis.

The three selected shell geometries which were taken for consideration purposes are shown in Figure 2. They are: (a) torispheres, (b) circular cylinders, and (c) truncated cones. Results are compared with available data in open literature.

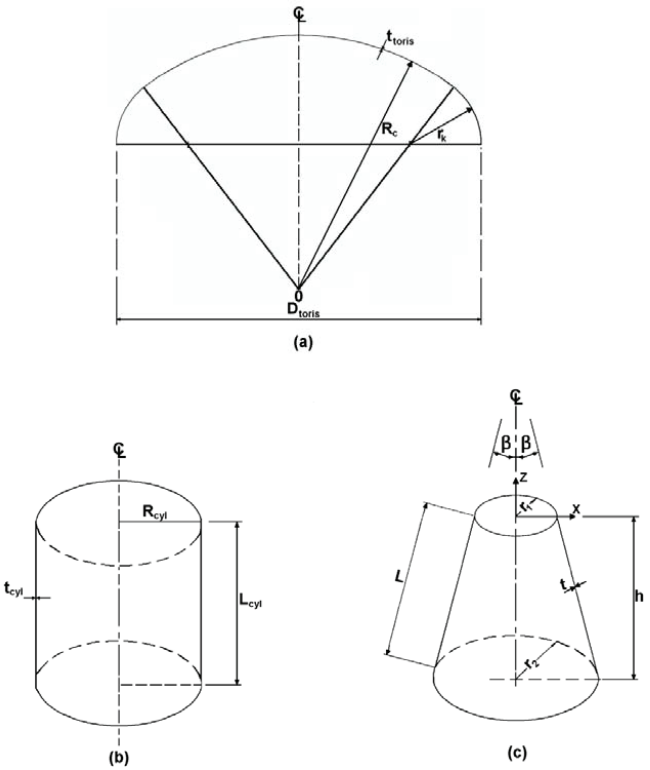

Figure 2. Geometry of: (a) torisphere, (b) circular cylinder and (c) truncated cone

2.1 Buckling and failure mode of externally pressurized torispheres

The structure illustrated here is a torisphere with crown radius, R_c, a knuckle radius, r_k, wall thickness, t_{toris}, and diameter of the base, D_{toris}, [see in Figure 2(a)]. Numerical calculations were carried out for: $R_c/D_{toris} = 1.0$, $r_k/D_{toris} = 0.2$ and $D_{toris}/t_{toris} = 500$. It is assumed that the torisphere is made from steel with the following material properties: Young's modulus, E = 207 GPa, Poisson's ratio, $\nu = 0.3$. Material of the torisphere was modeled as elastic. The structure was modeled using three dimensional shell elements (S8R) with eight nodes. Convergence studies presented in Table 1, shows that the grids of one hundred and twenty circumferential elements by forty meridional elements were sufficient.

Table 1. Convergence studies for externally pressurized torisphere, cylinder, and cone. (n/a ≡ not applicable)

Buckling	Mesh Density (Axial x Hoop) Elements						
Load (MPa)	40x40	40x60	40x80	40x120	40x160	60x60	80x60
Torisphere	0.6363	0.6232	0.6216	0.6211	0.6210	n/a	n/a
Cylinder	0.0181	0.0179	n/a	n/a	n/a	0.0179	0.0179
Cone	0.0856	0.0850	n/a	n/a	n/a	0.0850	0.0850

Next, the effect of using different preloading/perturbation magnitude is presented in Table 2. It can be seen from Table 2, that the magnitude of preloading/perturbation load used in the analysis has a significant effect on the bifurcation pressure of the torisphere. Then, the influence of using different boundary condition during the buckling analysis was investigated. Results are presented in Table 3. From Table 3, it can be noticed that changing the boundary condition at the end of the torisphere does not change the magnitude of the bifurcation pressure.

Table 2. Computed bifurcation buckling pressure corresponding to different preloading/perturbation magnitude for torisphere

Applied Load (MPa)		Bifurcation buckling
Dead load	Live load	Pressure (MPa)
0.3	0.03	0.7897 (11)
0.5	0.05	0.6211 (10)
0.52	0.052	0.5861 (10)
0.55	0.055	0.5858 (10)

Table 3. Comparison of computed bifurcation pressure corresponding to different boundary conditions at the base during buckling analysis, i.e.: (1) ≡ [$u_x \neq 0$, $u_y = 0$, $u_z = 0$, $\phi_x = 0$, $\phi_y = 0$, $\phi_z = 0$]; (2) ≡ [$u_x = 0$, $u_y \neq 0$, $u_z = 0$, $\phi_x = 0$, $\phi_y = 0$, $\phi_z = 0$]; (3) ≡ [$u_x = 0$, $u_y = 0$, $u_z \neq 0$, $\phi_x = 0$, $\phi_y = 0$, $\phi_z = 0$]; (4) ≡ [$u_x = 0$, $u_y = 0$, $u_z = 0$, $\phi_x \neq 0$, $\phi_y = 0$, $\phi_z = 0$]; (5) ≡ [$u_x = 0$, $u_y = 0$, $u_z = 0$, $\phi_x = 0$, $\phi_y \neq 0$, $\phi_z = 0$]; (6) ≡ [$u_x = 0$, $u_y = 0$, $u_z = 0$, $\phi_x = 0$, $\phi_y = 0$, $\phi_z \neq 0$]; (7) ≡ [$u_x = 0$, $u_y = 0$, $u_z = 0$, $\phi_x \neq 0$, $\phi_y \neq 0$, $\phi_z \neq 0$]; (8) ≡ [$u_x \neq 0$, $u_y \neq 0$, $u_z \neq 0$, $\phi_x = 0$, $\phi_y = 0$, $\phi_z = 0$]

Model	Bifurcation buckling pressure (MPa), with boundary condition at the base									
	(1)	(2)	(3)	(4)	(5)	(6)	(7)	(8)	Torisphere	0.65
0.65	0.65	0.65	0.65	0.65	0.65	0.65				
	(10)	(10)	(3)	(10)	(10)	(10)	(10)	(0)		

Model with fixed boundary condition at the base was then subjected to uniform external pressure. The preloading/perturbation magnitudes of 0.55 MPa / 0.055 MPa were used. Figure 3a depicts the shape of undeformed torisphere. The pre-buckling shape is shown in Figure 3b, and the buckling mode is presented in Figure 3c. It can be seen in Figure 3c, that buckling occurs at the junction between the crown and the knuckle.

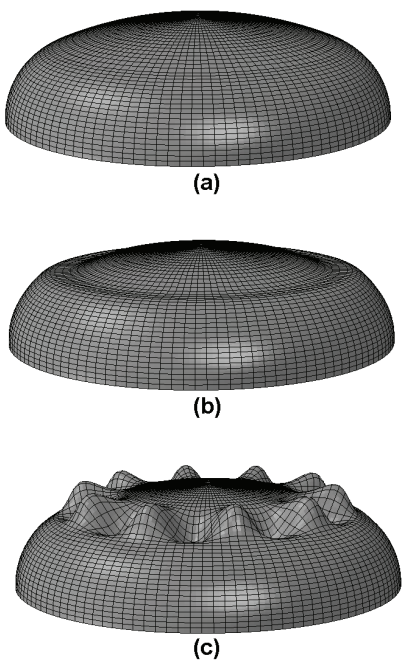

Figure 3. View of undeformed torisphere (Fig. 3a), deformed shape prior to buckling (Fig. 3b).The eigenshape, n = 10 (Fig. 3c)

The bifurcation buckling pressure, $p_{bif,}$ was found to be p_{bif} = 0.5858 MPa with n = 10 buckling waves in the circumferential direction. It is worth noting that collapse pressure is, p_{coll} = 0.7907 MPa. Exactly the same magnitudes of bifurcation pressure, p_{bif} = 0.58 (n = 10) MPa, and collapse pressure, p_{coll} = 0.8 MPa are given in (Blachut and Jaiswal, 1999). The numerical collapse pressure is in very close agreement with the experimental collapse pressure, p_{coll} = 0.835 MPa given in (Galletly et al., 1987). Figure 4 depicts the plot of external pressure against vertical apex deflection for a torisphere. Figure 4 indicates the position of the bifurcation pressure, p_{bif}, and the collapse pressure, p_{coll}.

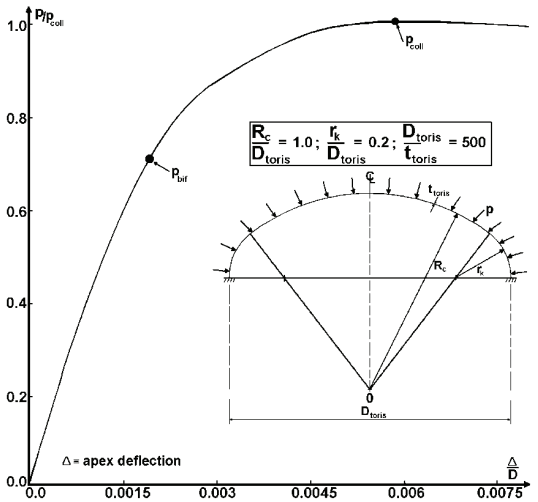

Figure 4. Plot of external pressure versus apex deflection for torisphere with R_c/D_{toris} = 1.0, r_k/D_{toris} = 0.2 and D_{toris}/t_{toris} = 500

2.2 Buckling and failure mode of externally pressurized circular cylinders

In this sub-section, a circular cylinder with radius, $R_{cyl,}$ uniform wall thickness, t_{cyl} and length, L_{cyl} as shown in Figure 2b will be examined for elastic buckling behavior. The geometry of the cylinder is L_{cyl}/R_{cyl} = 2, and R_{cyl}/t_{cyl} = 500. Material is considered to be elastic, with Young's modulus, E = 207 GPa and Poisson's ratio, ν = 0.3. The structure was model using three dimensional shell elements (S8R5) with eight nodes.

Convergence studies were carried out to determine the mesh density of the cylinder. Results obtained in terms of bifurcation pressure are presented in Table 1. From Table 1, FE grid of sixty hoop elements by sixty axial elements was chosen to be sufficient in modeling the cylinder. Changing the magnitude of the prebuckling/perturbation load does not influence the bifurcation pressure of the cylinder as given

in Table 4. Also, changing the boundary condition during the buckling analysis did not provide any convergent solution as shown in Table 5.

Table 4. Computed bifurcation buckling pressure corresponding to different preloading/perturbation magnitude for circular cylinder

Applied Load (MPa)		Bifurcation buckling
Dead load	Live load	Pressure (MPa)
0.01	0.001	0.01790 (9)
0.013	0.0013	0.01787 (9)
0.015	0.0015	0.01786 (9)
0.017	0.0017	0.01784 (9)

The preloading/perturbation magnitudes of 0.17 MPa / 0.017 MPa were used. The boundary conditions at the ends of the cylinder only allow axial movement while all other are restrained. It is worth noting here that the six different combinations of boundary conditions in Table 5 do not cover the boundary condition used at the ends of the cylinder for estimating the bifurcation pressure of the circular cylinder.

Table 5. Comparison of computed bifurcation pressure corresponding to different boundary conditions at the top and bottom edges during buckling analysis for different cases, i.e.: (i) ≡ [ux = 0, uy = 0, uz = 0, ϕx = 0, $\phi_y = 0$, $\phi_z = 0$]; (ii) ≡ [$u_x = 0$, $u_y = 0$, $u_z = 0$, $\phi_x \neq 0$, $\phi_y \neq 0$, $\phi_z \neq 0$]; (iii) ≡ [$u_x \neq 0$, $u_y \neq 0$, $u_z \neq 0$, $\phi_x = 0$, $\phi_y = 0$, $\phi_z = 0$]; (iv) ≡ [$u_x \neq 0$, $u_y \neq 0$, $u_z \neq 0$, $\phi_x \neq 0$, $\phi_y \neq 0$, $\phi_z \neq 0$]. Note: * ≡ No convergent solution

Boundary	Top	(iv)	(i)	(ii)	(iii)	(iv)	(iv)
Conditions	Bottom	(i)	(iv)	(iv)	(iv)	(ii)	(iii)
Bifurcation	Cylinder	*	*	*	*	*	*
Pressure (MPa)	Cone	0.085(8)	*	*	*	0.085(8)	*

Figure 5a, Figure 5b and Figure 5c depict the undeformed shape, prebuckling shape and the buckling mode of the cylinder, respectively. It can be seen from Figure 5c, that the cylinder fails by the formation of lobes around the circumference with 9 waves, at a bifurcation pressure, pbif, of 0.017839 MPa. These results compare well with the magnitude of numerical bifurcation pressure, p_{bif} = 0.017796 MPa and wave number, n = 9, given in (Figure 3 of Blachut, 1987). Exactly the same magnitude of experimental bifurcation pressure, p_{bif} = 0.0183 (n = 9) MPa was reported in Table 1 (Fakhim et al., 2009).

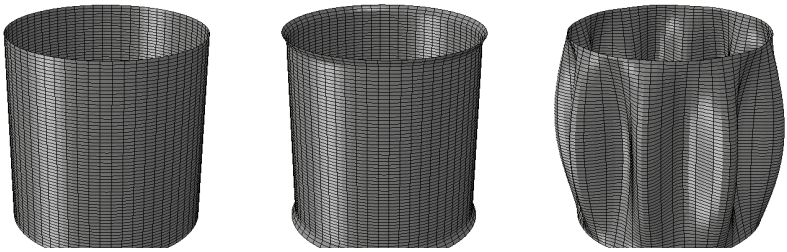

Figure 5. View of initial FE model (Fig. 5a), the prebuckling shape (Fig. 5b), and buckling mode, n = 9 (Fig. 5c). Note: Cylinder is subjected to external hydrostatic pressure

2.3 Buckling and failure mode of externally pressurized truncated cones

Consider a truncated cone with radii, r_1 and r_2, and uniform wall thickness, t, having the height given by, h, cone slant length, L and semi-vertex angle, β, as sketched in Figure 2c. Let the geometric parameters be given as: $r_2/t = 393.7$, $r_2/r_1 = 5$, $h/r_2 = 2.198$ and $\beta = 20^0$. It is assumed that the cone is made from mild steel, and the following material properties are used for numerical calculations: Young's modulus, E = 210 GPa, Poisson's ratio, $\nu = 0.3$. Three dimensional shell elements with eight nodes (S8R5) are to be used.

Results obtained from convergence studies are presented in Table 1. Convergence studies shows that FE grid of sixty S8R5 elements in the circumferential direction and sixty S8R5 elements in the axial direction were sufficient. The effects of using different preloading/perturbation magnitudes do not change the bifurcation pressure as can be seen in Table 6. Also, presented in Table 5 is the effect of using different boundary conditions during the buckling analysis.

Table 6. Computed bifurcation buckling pressure corresponding to different preloading/perturbation magnitude for truncated cone

Applied Load (MPa)		Bifurcation buckling
Dead load	Live load	Pressure (MPa)
0.02	0.002	0.0846 (8)
0.04	0.004	0.0849 (8)
0.06	0.006	0.0851 (8)
0.08	0.008	0.0853 (8)

From Table 5, it can be observed that in order to obtain a convergent solution, displacement degree of freedom must be specified at the bottom edge. Therefore, model with fixed boundary conditions at both top and bottom edges of the cone were subjected to uniform external pressure. Also, it must be noted that the six different combinations in Table 5 do not cover the boundary condition used at the ends of the cone for determining its bifurcation pressure. The preloading/perturbation magnitudes of 0.08 MPa / 0.008 MPa were used.

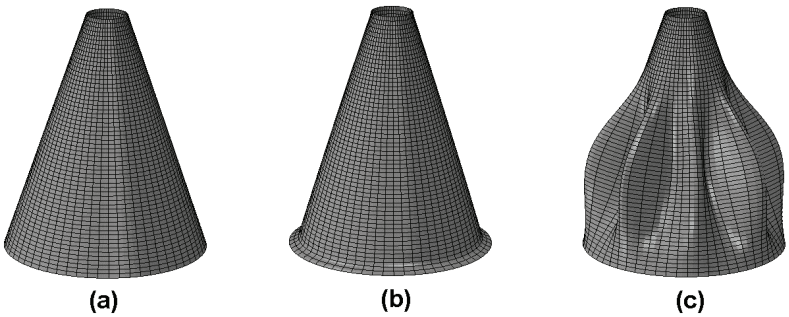

Figure 6. View of initial undeformed model (Fig. 6a), deformed shape prior to buckling (Fig. 6b), and the eigenshape with n = 8 circumferential lobes at bifurcation (Fig. 6c)

Figure 6a depicts the initial shape of the cone prior to external pressure loading. The shape of cone prior to buckling is presented in Figure 6b, whereas, the deformed shape of the cone at buckling is shown in Figure 6c. It is seen in Figure 6c that the cone fails with asymmetric bifurcation load of 0.08534 MPa, with the eigenshape corresponding to n = 8 circumferential waves. These results compare well with the magnitude of bifurcation pressure, pbif = 0.086 MPa and wave number, n = 8, presented in (Table 2 of Blachut, 2011).

3.0 CONCLUSIONS

Bifurcation buckling strength of three major structural shell components i.e., torisphere, cylinder and cone has been considered. The effect of using different magnitude of prebuckling/perturbation load and variability of boundary conditions at the ends has been highlighted. Based on this contribution, a number of conclusions can be drawn. They are that: (i) for the case of torisphere, results indicate that the magnitude of prebuckling/pertubation load has significant effects on the bifurcation pressure, whilst, changing the edge support has no effect on the buckling load, and (ii) for the case of circular cylinder and cone, numerical calculation reveals that the magnitude of the prebuckling/

pertubation load does not affect bifurcation pressure, whereas, in the case of variability of edge support, it is practically impossible to obtain a convergent, except the edge support specified is either pinned or fully clamped at both ends. This study offer only a limited insight into the bifurcation buckling behaviour of these three shell structures. Past study on plastic collapse of cones has found that there is always a collapse load obtained for these boundary conditions. Hence, further work on the effect of prebuckling load and variabilty of edge support on these shell structures for different geometry, i.e., radius-to-thickness ratio would be desirable.

4.0 REFERENCES

Blachut, J. (1987). Combined axial and pressure buckling of shells having optimal positive gaussian curvature, *Computers and Structures, 26*(3), 513-519.

Blachut, J. (2011). On elastic-plastic buckling of cones, *Thin-Walled Structures, 49*(1),45-52.

Blachut, J., Jaiswal, O. R. (1999). Instabilities in torispheres and toroids under suddenlyApplied external pressure, *International Journal of Impact Engineering, 22*(5), 511-530.

Fakhim, Y.G., Showkati, H., Abed, K. (2009). Experimental study on the buckling and post buckling behavior of thin-walled cylindrical shells with varying thickness under hydrostatic pressure, Alberto Domingo and Carlos Lazaro (eds.), P*roceedings of the International Association for Shell and Spatial Structures (IASS)* Symposium 2009, 28 September – 2 October 2009, Valencia, Spain.

Fung, Y. C. & Sechler, E. E., (1974). The historic development of shell research and design, in Thin-Shell Structures, Theory, Experiments and Design, Englewood Cliffs, N.J: Prentice Hall.

Galletly, G.D., Kruzelecki, J., Moffat, D.G., Warrington, B. (1987). Buckling of shallow torispherical domes subjected external pressure - a comparison of experiments, theory and design codes, *The Journal of Strain Analysis for Engineering Design, 22*(3), 163-175.

Hibbitt, Karlsson, Sorensen. (2006). ABAQUS-*Theory and Standard User's Manual Version* 6.4, USA, Pawtucket.

Ifayefunmi, O. (2011). *Combined stability of conical shells*, (unpublished PhD Thesis), University of Liverpool, Liverpool.

Ifayefunmi, O., Blachut, J. (2011). The Effect of Shape, Boundary and Thickness Imperfections on Plastic Buckling of Cones, *Proceedings of the ASME 2011 30th International Conference on Ocean, Offshore and*

Arctic Engineering. NY, USA: Vol. 2, OMAE2011-49055, 2011, pp. 23-33, ASME

Kyriakides, S., Corona, E. (2007). *Mechanics of Offshore Pipelines*, Vol. 1: *Buckling and Collapse*, (1st Ed) Oxford, UK: Elsevier BV.

Nash, W. A. (1960). Recent advances in the buckling of thin shells, *Applied Mechanics Review, 13*(9), 161-164.

Noor, A. K., (1990). Bibliography of monographs and surveys of shells, *Applied Mechanics Review, 43*(9), 223.

Samuelson, L. A., Eggwertz, S., (1992). *Shell Stability Handbook.* Essex, UK: Elsevier Science Publishers Ltd,

Singer, J. (1999). On the importance of shell buckling experiments, Applied Mechanics Review, 52(6), R17 – R25.

Singer, J., Arbocz, J., and Weller, T. (2002). Buckling Experiments: Experimental Methods in Buckling of Thin-Walled Structures, Volume 2, Wiley, New York.

Teng, J. G., Rotter, J. M., (2004). *Buckling of thin shells, in Buckling of Thin Metal Shells*, J. G. Teng, J. M. Rotter (eds), Spon Press, London